Journal of Engineering Science and Technology
Special Issue on SIET2022, May (2022) 214 - 241

SMART ENERGY PERFORMANCE IMPROVEMENT ON PHOTOVOLTAIC (PV) SYSTEM

TING Z. LAM[1], ZAIN K. USMANI[1], ALI MINAAH[1],
CHONG P. KHEY[1], SALEH M. A. QASHMAR[1], SURESH GOBEE[2],
VICKNESWARI DURAIRAJAH[2]

[1]School of Engineering, Asia Pacific University of
Technology and Innovation, Bukit Jalil, 57000 Kuala Lumpur, Malaysia
[2]Faculty of Computing, Engineering & Technology, Asia Pacific University of Technology
and Innovation, Bukit Jalil, 57000 Kuala Lumpur, Malaysia
*Corresponding Author: suresh.gobee@apu.edu.my

Abstract

To reduce the environment pollution due to the heavy dependency on fossil fuel in energy production, solar energy been investigated to encourage public on using the renewable energy. The current photovoltaic (PV) system is sensitive to temperature, and it cannot exhibit the maximum efficiency with external factors such as partial shading, shadow casting, indirect sunlight and accumulating dusts on the solar panel. There is also lesser Internet of Things (IoT) interface application for users to monitor the solar panel condition. The project aims to innovate an efficiency PV system with the implementation of sensor-less solar tracking, algorithmic self-cooling, integrated electronics and IoT system. The system developed integrated DC-DC Converter with Maximum Power Point Tracking (MPPT) algorithm to track the maximum power point (MPP) of the panel and construct a motorized platform for the PV panel in conjunction with the solar tracking and self-cooling capability. An application that monitors the parameters of the PV panel is also developed. The result of the final developed system is having 25.22% efficiency increment.

Keywords: Dual-axis solar tracking, IoT with blynk, Motorized tracking platform, MPPT, Panel cooling system.

1. Introduction

As renewable energy becomes a solution due to humans heavily depending on the non-renewable energy sources, the alternative and cleaner energy needs to be applicable to people with different level of needs. The usage of non-renewable energy has harmed the environment that provides life for humans, and thus the project will be focusing on enlarging the solar energy that is harvested from the sun through the usage of dual axis solar panel structure.

To understand how the solar power can be introduced to the residential and industrial application, firstly, the solar panels will be fabricated with the array of photovoltaic cells, and the PV cells will convert the solar irradiation from sunlight to proportional DC voltage output, as shown in Fig. 1. Then, it is fed into the charge controller that manages safely on the battery charges that store the energy that is harvested from solar panels. After that, the system gets connected to the existing electrical grid, as shown in Fig. 2.

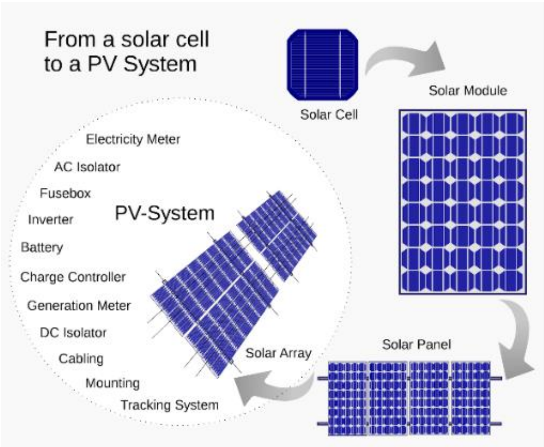

Fig. 1. PV system formation.

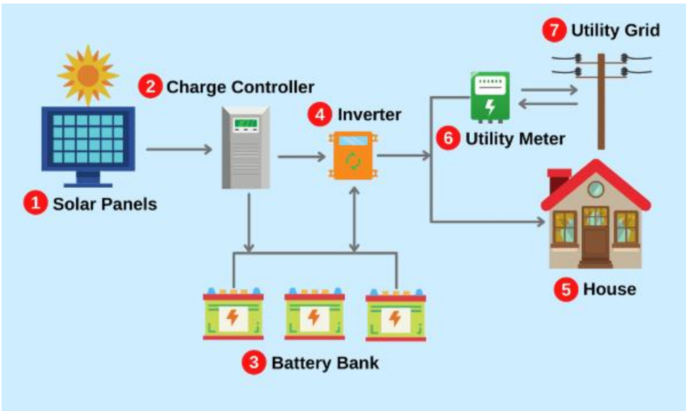

Fig. 2. Flow of electrical power.

The system has several flaws that diminishes the renewable energy being widely utilized in the society nowadays. Kurpaska et al. [1] showed that the performance of the solar panel is very sensitive to increase in temperature, and every 50 ℃ rises in temperature will cause a 20.1% drop in the efficiency of PV module. Secondly, the system has high dependency to changes of environment. Kazem et al. [2] found out that shadow casting on panel surface, indirect sunlight, and accumulated dirt on the solar panel will lower the efficiency exponentially.

Kazem et al. [2] pointed out that PV systems does not have a user-friendly and modern IoT implementation as shown in Fig. 3.

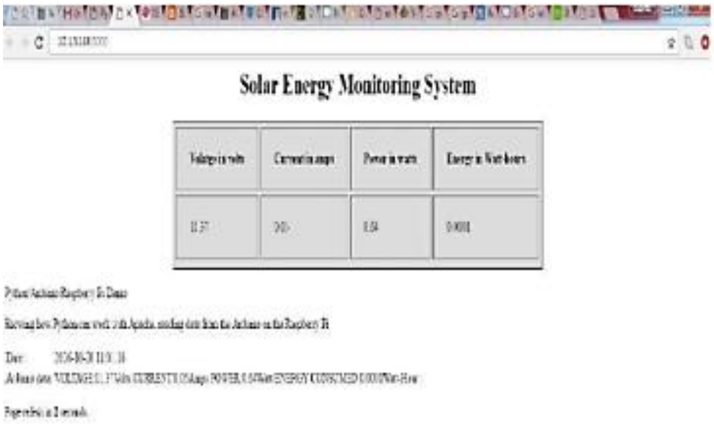

Fig. 3. IoT system dashboard [2].

Along with traditional energy sources, the importance of renewable energy as a key source of energy for the entire world has gradually grown. The energy requirements have increased rapidly as a result of their development. Solar PV systems, on the other hand, are not always efficient as we would like. Also, solar panels do not perform consistently in all settings, and several factors can reduce efficiency. Thus, this study was conducted in order to improve solar panel efficiency and acquire the highest potential electricity output.

On the other hand, most of solar panel systems are missing the smart energy management system [3] This makes it difficult for the user to know if the solar panel efficiency is good or not. Thus, this study improved the system with remote data monitoring by using energy meters and IoT gateways, as well as the system, allowing the user to control the system from anywhere [4].

2. Support Platform Design

2.1. Platform design investigation

The solar tracking structure design is important in ensuring the solar panel and cooling system can be properly supported with the weight of components. The stability of the solar panel platform must be considered as the project will need the platform to always move in incremental motion. The structure must be practical by using the material wisely, and a compact design for a lesser carbon footprint produced. Lastly, the platform created must consider being hassle-free as the design consists of wiring and testing, thus a platform that is simple and functional is considered. The azimuth is the motion that turns the platform horizontally, while the elevation, or the tilt, is the motion that turns the solar panel in angular motion.

In the first design, Fig. 4, two gears on the bottom functions as the azimuth by turning the middle rod that supports the solar panel. The top two gears functions as the tilt of the solar panel platform by turning the rod that's connected to the thinner rod that determines the solar panel facing direction. The solar panel has 4 attachments that are connected, which will fasten the linkage between the tinner rod and solar panel, thus allowing the entire system to function as a dual-axis solar panel platform structure.

The second design, as in Fig. 5, utilizes two sets of racks and pinion to function as a tilt for the solar panel, and an extra motor at the bottom to act as the function of azimuth. There is an increase of the attachments with the rod. The solar panel placement has a design to ensure the platform does not drop by fixating it with the outer design frame. These designs contribute to how the design above satisfies the platform in becoming a dual-axis solar panel platform. The utilization of rack and pinion can be likened to the working of a linear actuator where the elevation of the solar panel can be adjusted precisely.

The project focuses on constructing a motorised solar panel structure platform that can apply solar tracking and cooling capabilities. The tabulated data shown in Table 1 shows that the materials utilized by the second design will be higher. The gears, rod supporter, and solar panel frame of design 2 will increase the cost of the project, as more materials will be used to design, assess, and recalibrate to ensure the prototype is stable and can perform the expected tasks. Secondly, the structural stability of design two is lesser than design 1, as design 1 applied a more straightforward method to have both the functions of azimuth and elevation. Design 2 utilizes rack and pinion, which, though it is a workable idea since it provides a rotation to linear motion, the stability of rack and pinion must be further explored, as the structure posed only allows a certain angle of solar panel to be tilted. The longer the rack, the more the elevation of the solar panel can be controlled. Thirdly, viewing from the materials and structure of both designs, the material used for design 1 is lower than for design 2. Since the prototype constructed will be redesigned to perfect the platform, it is suggested that design 1 is to be further improvised and testing will be done to save cost used in the project and reduce the complexity of the design. Thus, design 1 is chosen as the fundamental design to be enhanced.

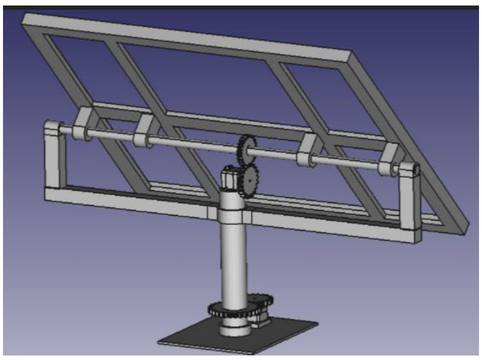

Fig. 4. Solar panel platform design 1.

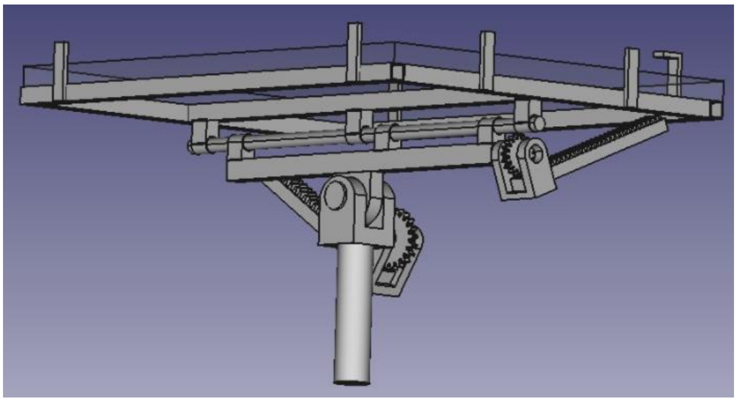

Fig. 5. Solar panel platform design 2.

Table 1. Solar panel structure material design comparison.

Parameters	Design 1	Design 2
Gears	4 (spur gears)	2 sets of rack and pinion
Rod	2	2
Rod supporter	1 (6 attachments)	2 (6 attachments)
Solar panel frame	0 (to use solar panel for fitting)	1
Motor	2	3

2.2. Design of platform and testing

The design of the platform as in Fig. 6 is firstly to have a strong double-sided tape to tape the solar panel to the support holder. Then, the thick rod holder supports the weight of the panel and motor. The thick rod supporter supports the abovementioned structure, and then the small support platform will help to spin the thick rod with respect to the gear for lesser friction force occurring. The excess space at the thinner rod above is to make space for cooling components and wirings. The platform below everything is to support and stabilize the entire platform.

This position is when the stress and strain of the entire platform are at their maximum point. The external forces are gravity and the solar panel's weight. From the Finite Element Analysis in SOLIDWORKS as in Fig. 7, the middle rod that links the gears and the solar panel will experience high stress and strain.

Figure 8 shows Displacement Analysis of the structure, though it shows that the solar panel will have a displacement, however, the actually affected component will be the thin rod.

To reduce the stresses that will cause deformation during the prototype production, the stepper motor setup can help to reduce the straining of the rod as it connects to the gear. The linkage of the rod and platform is designed with a hexagon and infill of 25%

for all parts except the gears and the thin rod, as shown in Fig. 9. The support platform has also been redesigned for a larger area to support the solar panel.

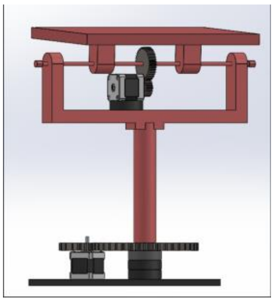

Fig. 6. Finalized platform design.

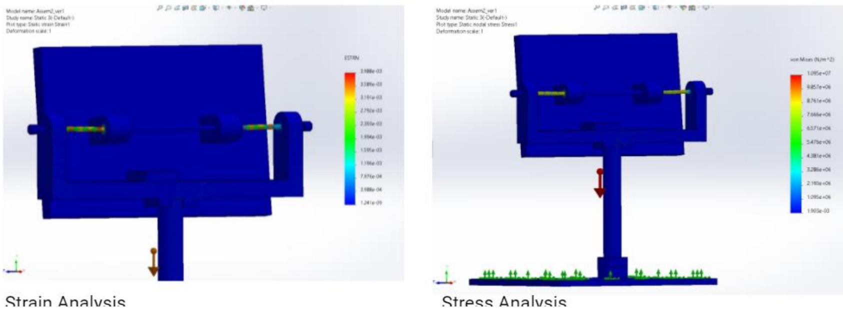

Fig. 7. Stress and strain analysis of platform.

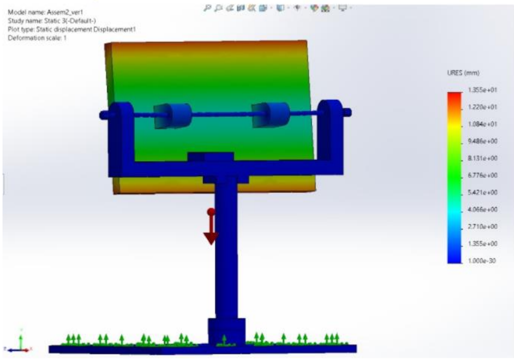

Fig. 8. Displacement analysis of platform.

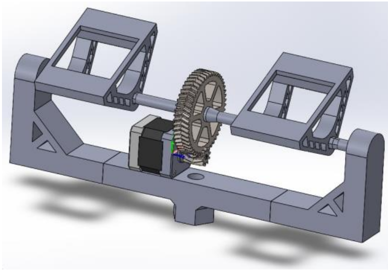

Fig. 9. New design of top solar panel platform.

3. Cooling Design

3.1. Cooling design investigation

Solar cells like all other semiconductor devices, are temperature sensitive. Temperature increases diminish the bandgap of a semiconductor, affecting the majority of its material properties. As a result, less energy is required to break the connection. A decrease in the bond energy reduces the bandgap in the bond model of a semiconductor bandgap. As a result, raising the temperature lowers the bandgap. Figure 10 shows the effect of rising temperatures on the open-circuit voltage. Because I0 is temperature-dependent, the open-circuit voltage drops with the temperature [5].

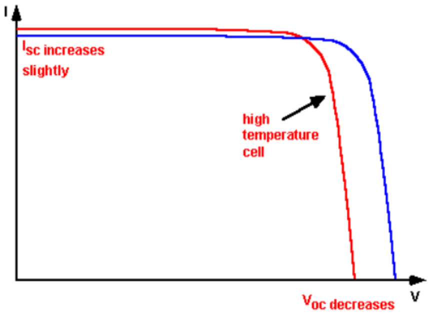

Fig. 10. The effect of temperature on I and V of PV [5].

Frequently, solar panels are tested at 25 degrees Celsius (77 degrees Fahrenheit), so the optimal temperature for solar cells is between 15 and 35 degrees Celsius. Solar panels, on the other hand, may reach temperatures of up to 65 degrees Celsius (149 degrees Fahrenheit), at which time solar cell efficiency suffers [6]. The temperature coefficient of any solar panel can be between 0.3% and 0.5% which uses to calculate the power loss. one example will be taken when the temperature is 50 °C for the solar panel that has a temperature coefficient of 0.35% [7]:

- Firstly, the difference in temperature between the normal testing temperature of 25 °C and the actual temperature which is assumed as 50 °C.

$$\Delta T = T_N - T_A \quad (1)$$

$$50°C - 25°C = 25°C$$

- Then, the difference in temperature multiples with temperature coefficient of 0.35%

$25℃ * 0.35\% = 8.75\%$

- Thus, the power is losing by 8.75 percentage at temperature 50 ℃

This chapter discusses various cooling approaches that can be used to lower the operating temperature of PV cells. Where it will include an investigation of tools and techniques that used to implement the cooling system, proposed cooling system methodology, and concept design of the system, and how the system is implemented in both simulation and prototyping.

The goal of this chapter is to improve the performance of PV systems by keeping cell temperatures as low as possible. as it is known that the operating temperature influences the efficiency of solar panels. Where increasing the temperature of a solar cell reduces its efficiency. Thus, a cooling system must be included for this project to keep the PV cell temperature constant to improve efficiency.

3.2. Design of cooling system

Fig. **11** shows the block diagram of the cooling system. The temperature is read by the thermistor sensor which connect to the microcontroller. In the system, two fans and water pump will be used to cool down the solar penal as the water pump push the cold water to be solar panel. The fans produce a cool air around the solar penal where it helps the solar penal to cool down. LCD screen will be used in simulation to display the temperature degree which will be displayed integral system in the application.

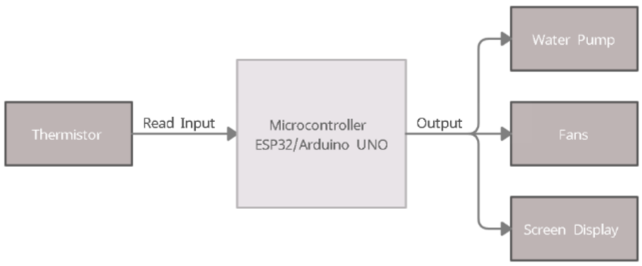

Fig. 11. Block diagram of cooling system.

Fig. **12** shows the flow chart of the cooling system. The system starts operating by reading temperature value of the solar panel. Based on the reading temperature the cooling system will be activated. When the temperature between 34 ℃ and 37 ℃ the fan will be activated. When the temperature above 37 ℃ the water pump will be activated. Else when the system less than 34 ℃ all of fans and water pump will be deactivate. The conditions of the system were developed based on the average temperature of Malaysia and the different in temperature of the solar penal and air. [8]

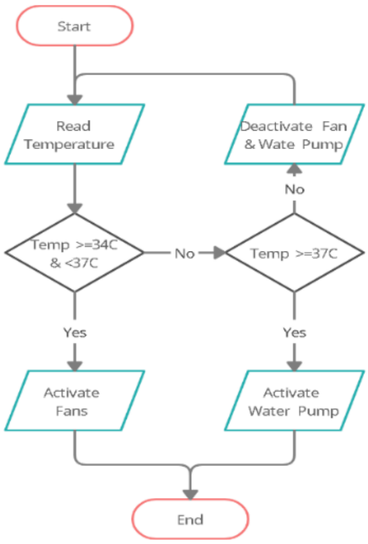

Fig. 12. Cooling system flow chart.

The algorithm conditions that control the cooling system way are defined based on the average temperature of Malaysia and the difference in the temperature of the solar panel and air. Where Malaysia's average daily temperature ranges from 21 °C to 32 °C [8], and the average value difference in temperature of the air and solar panel that it can be found using the following equation:

$$\Delta T = |T_{cell} - T_{air}| \tag{2}$$

where the T_{cell} can be calculated by using the equation below. It is used to develop the temperature conditions of the algorithm only. In the real prototype, the T_{cell} is a measured temperature that will be read by the thermistor only.

$$T_{cell} = T_{air} + \frac{NOCT-20}{800}S \tag{3}$$

where:

- NOCT is the normal operation cell temperature of the PV panel.
- S is the Solar Irradiance in W/cm^2.

To calculate the maximum cell temperature, a maximum temperature that can be reached in Malaysia is used which is 32 °C. Assume that the highest temperature can be the solar panel measure is when the sun’s ray in straight line into the solar surface which can be 1100 W/cm^2. The NOCT of solar penal that used is 25 °C.

$$T_{cell(\max)} = 32 + \frac{25-20}{800}1100 = 38.8\ ℃$$

As it was mentioned in the investigation that the solar penal reach to the best efficiency when the temperature between 15 °C and 35 °C. based on this value temperature condition was developed where when the temperature is 34 °C going to 35 °C the cooling fans activate to keep the temperature less than 35 °C. In case if the temperature goes to maxim above 38 °C, the water pump is activated where the water is better that the air in heat transfer. Water is used to keep the temperature less than 37 °C.

Thermistor is a resister that effects by a temperature refer to Fig. 13 as the relation between them can be found by the following equation:

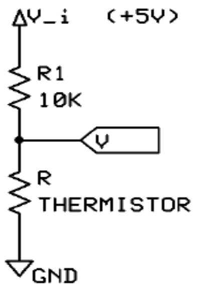

Fig. 13. Voltage divider circuit of the thermistor.

For Eq. (4), the R is the thermistor resistor, R_1 is the fixed resistor, which is 10 K ohm, B is the constant, which is 3380, and T_r is the normal temperature of 25 °C. T is the temperature of the solar that it will be measured.

$$R = R_1 \exp\left(B\left(\frac{1}{T} - \frac{1}{T_r}\right)\right) \tag{4}$$

Which can be found by following equation:

$$T = \frac{1}{T_r} + \frac{1}{B}\, In\left(\frac{R}{R_1}\right)^{-1} \tag{5}$$

$$T = \frac{1}{25} + \frac{1}{3380}\, In\left(\frac{R}{10k}\right)^{-1}$$

Firstly, R must be found. Based on the voltage divider circuit R can be found from the following Equation.:

$$V = \frac{R1}{R1+R} Vi \tag{6}$$

where the V is the reading voltage which connects into the microcontroller. Vi is the voltage that input to the divider circuit which is 5 V for Arduino UNO and 3.3 V for the ESP32 microcontroller. So, R is equal to:

$$R = \frac{5 * 10k}{V} - 10k$$

$$R = \left(\frac{5 * 10k}{V} - 1\right)$$

The above equation will be used in Arduino code. Where the v is collecting data and the 5 with red colour can be changed based on the working voltage of the microcontroller, 5 V for Arduino Uno with ADC of 1023, and 3.3 V for ESP32 with ADC of 4095.

As discussed above, the reason for using a switch to operate the fan and water pump. As N-MOSFET was selected to be used. Figure 14 shows how MOSFET- Fan/Pump circuit is connected. Where a resistor of 100 ohm is connected between the output pin from the microcontroller into the MOSFET gate part to limit the current. Where resistor of10 K ohm is connected between the ground and gate part in case if the microcontroller has any problem the voltage will be grounded to off the fan or pump. Diode connects in parallel with the fan/pump to avoid any damage can be for the MOSFET which can be burned by the high voltage that happens when the fan switches off.

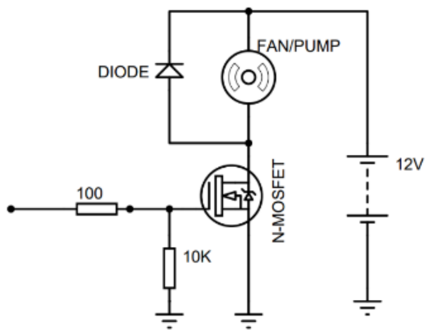

Fig. 14. Transistor switch circuit for fan and water pump.

4. Microcontroller Design for Solar Tracker

4.1. Solar tracker investigation

Solar tracking, which refers to tracking the position of the sun on the sky, has been implemented in various PV systems over the years. Specifically, the PV panel is oriented to point directly at the sun to maximize the amount of solar irradiation striking the surface of the panel; thereby resulting in greater power output from the system. The solar irradiation impacting on Earth from the sun consists of two components - namely "direct" and "diffuse". The direct component delivers the maximum amount of solar energy as the beams are originated directly from the sun itself. The diffuse component, on the other hand, occupies a very low percentage of the total solar energy as they are essentially sunlight that has been scattered in all directions in the atmosphere. Therefore, the prime function for a solar tracker is to capture the maximum available direct component by minimizing the cosine effect. The cosine effect refers to the reduction of effective surface area (that could harvest solar energy) due to the incidence angle formed between the sunlight and the normal line of the PV panel [8], as shown in Fig. 15.

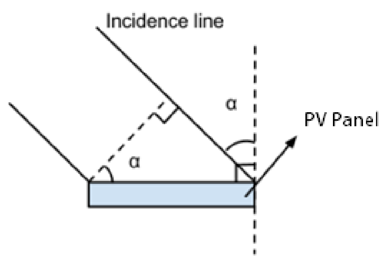

Fig. 15. Definition of the Cosine effect [8].

As evident from Fig. 15, the cosine of the incidence angle represents the ratio between the effective surface area and the actual surface area of the PV panel. Therefore, as the incidence angle decreases, the effective area (and thus the solar energy harvested) is increased.

Fig. **16** illustrates the power lost due to the cosine effect as the angle of incidence is swept from 0 to 90°. From this semi-log graph, it is clear that the power loss approaches zero as the angle of incidence is close to 0°, which is the ideal alignment. Additionally, it is evident that even a 25° degrees misalignment drops the direct power by 10%.

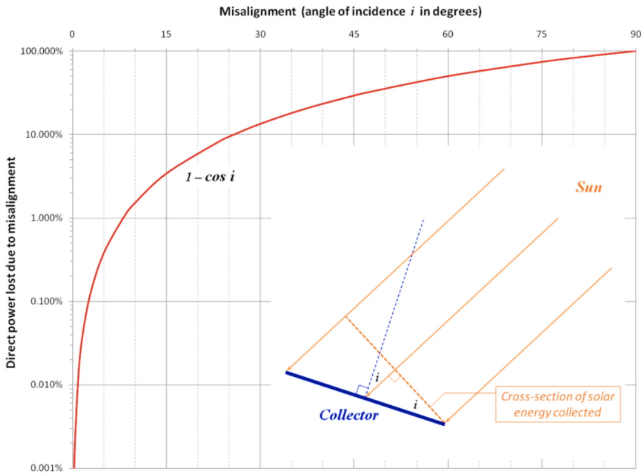

Fig. 16. Relationship between misalignment of PV panel and power loss [9].

There are several types of solar trackers that have been developed by researchers. Traditionally, solar tracking was performed manually by changing the orientation of solar panels at regular time intervals throughout the day. Nowadays however, with the advancement of technology, this process is automated using microcontrollers and actuators. When it comes to automated solar tracking, either closed-loop or open-loop control is implemented. The closed-loop approach utilizes an array of photoelectric sensors to detect the brightest source of light and provides feedback to the microcontroller. This technique does not guarantee that the panel is always perfectly aligned for minimal cosine effect. In addition, it is also susceptible to errors that may occur due to: (i) degradation of sensor quality (possibly due to the accumulation of dust and grime) and (ii) objects in the environment blocking the sensors.

A better approach is open-loop control, which will be implemented in this project, whereby the exact position of the sun is calculated using highly accurate astronomical formulae without relying on delicate sensor hardware. This technique ensures that the PV panel is always oriented directly at the sun, irrespective of the environmental conditions.

The path taken by the sun on the sky varies dramatically depending on two major factors – the time of the year and the location on earth. This can be illustrated on a sun path diagram, which is a 2D projection of the sky dome whereby the center of the plot is directly overhead with 90° elevation and the outer-most circle represents the horizon. The yellow shaded area in **Error! Reference source not found.** shows the a nnual variation in the sun path for Kuala Lumpur. It is evident that the sun does not follow the same path throughout the year, thus a robust solar tracking algorithm that accounts for these variations is necessary for the best results.

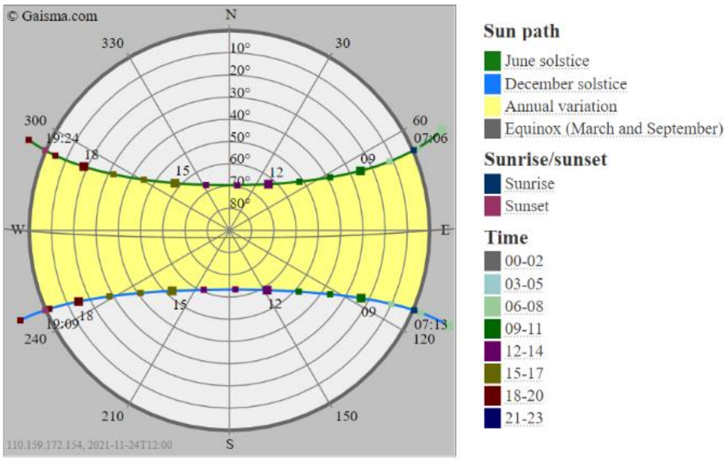

Fig. 17. Sunpath diagram for Kuala Lumpur.

When it comes to practical implementation of solar trackers, there are two different mechanisms used – single axis and dual axis solar trackers. Single axis solar trackers are capable of tracking the sun on a single axis (either solar elevation or azimuth). Typically, the elevation of the PV panel is fixed while solar tracking is executed on the azimuthal axis i.e., tracking the sun along the east-west direction. Dual axis solar trackers offer a superior level of solar tracking as they can track the sun in two axes (both solar elevation above the horizon and azimuth). Therefore, the sun is precisely tracked exactly as predicted by sun path diagrams.

4.2. Design of solar tracker

Fig. **18** shows the general block diagram of the proposed methodology to develop the sensor-less open loop solar tracking system. The block diagram illustrates the architecture of the proposed methodology with ESP-32 development board as the microcontroller unit and its associated peripheral inputs and outputs.

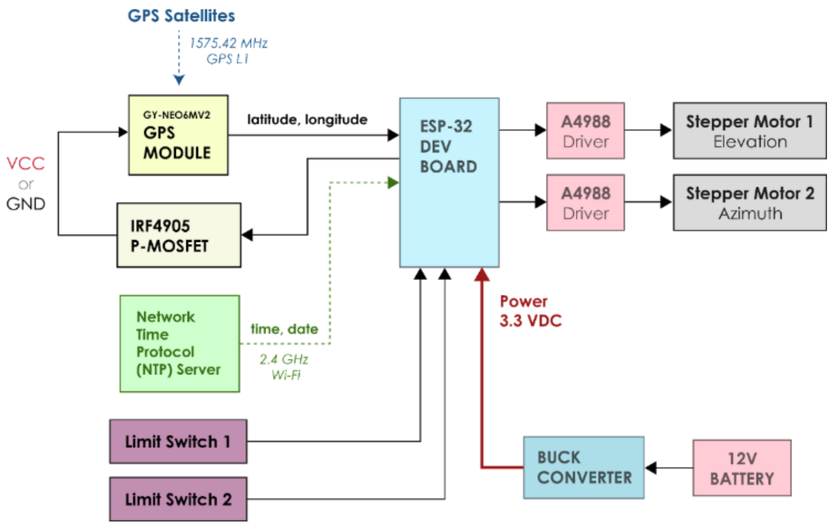

Fig. 18. Block diagram for solar tracking system.

The first input to the system is the GY-NEO6MV2 GPS module that automatically outputs geolocation data (current latitude and longitude) with serial communication to the ESP-32. The module automatically captures several GPS satellites and communicates with them via GPS L1 frequency (1575.42 MHz) to calculate the exact location based on triangulation technique.

An enhancement will be implemented which uses a P-channel MOSFET (specifically, the IRF4905 PMOS transistor) to control the power supply to the GPS module according to signals output by the ESP-32. This feature would allow the microcontroller to completely switch off the GPS module right after the location is obtained; thereby minimizing the power consumption of the system and subsequently, reduce the rate of battery discharge. Next, the ESP-32 would connect to the specified Wi-Fi network and communicate with the NTP (Network Time Protocol) server to retrieve the current date and time information. With these two inputs (geolocation, date & time), the ESP-32 would execute the solar position calculating algorithm to calculate the current solar elevation and azimuth angles, as shown in Fig. 19.

As depicted in Fig. 19, the solar elevation angle is defined to be the vertical angle formed between the horizon and the sun. Additionally, the solar azimuth angle is defined to be the horizontal angle formed between due North and the sun. This is essentially the “compass direction” of the sun, and it is measured clockwise from North. Once the current solar elevation and azimuth angles are calculated by ESP-32, it will calculate the required number of steps for both stepper motors in order to tilt and turn the PV panel in both axes. As a result, control signals are output to the two stepper motor drivers (A4988) – one for each axis. The drivers convert the control signals into appropriate driving signals to step (rotate) the stepper motors as required.

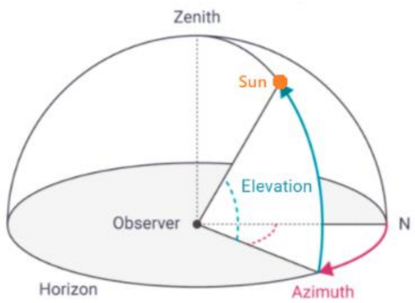

Fig. 19. Definition of solar elevation and Azimuth angles.

Other than that, two limit switches are also used as inputs to the system. These limit switches are essential to ensure accurate and repeatable positioning of the PV panel since stepper motors are inherently open loop devices with no positional feedback associated with them (unlike servomotors). As the system is first powered up, both stepper motors will be stepped in reverse direction slowly until the limit switches are activated. This sequence is known as “homing” and it ensures both stepper motors are at the home position (0°) before tracking is initiated. The prototype will have limit switches attached in appropriate positions such that the PV panel initially points to the horizon at 0° elevation and due North at 0° azimuth.

The entire system is self-powered by the 12 V battery that stores harvested solar energy with the electrical system. A DC-DC buck converter is used to step down the voltage to 3.3 V, which is appropriate for the ESP-32.

Fig. **20** shows a simplified flow of the proposed methodology that will programmed into the ESP-32 microcontroller. The flowchart consists of sub-algorithms that have been simplified to one block to clearly illustrate the main algorithm for pedagogic purposes.

The flow of the system begins by homing the stepper motors to ensure the PV panel is pointing at the horizon due north at the beginning. This is to ensure accurate positioning of the panel as stepper motors lack positional feedback, as explained earlier. Next, the GPS module is turned on by activating the PMOS transistor. As the GPS module is turned on, it automatically begins searching for available satellites in the sky. Once sufficient satellites have been captured, the geolocation is accurately triangulated and transmitted to the ESP-32 microcontroller via serial communication. This process takes some time, depending on various factors such as cloudiness of the sky and antenna placement. One limitation of the GPS module is that it requires direct line of sight to the satellites outdoors, however this is not a problem in this application as the PV panel will always be placed outdoors. Once the geolocation data has been obtained, the latitude and longitude variables are updated internally, and ESP-32 connects to the specified Wi-Fi network. It then communicates with the NTP server to retrieve the current date and time information.

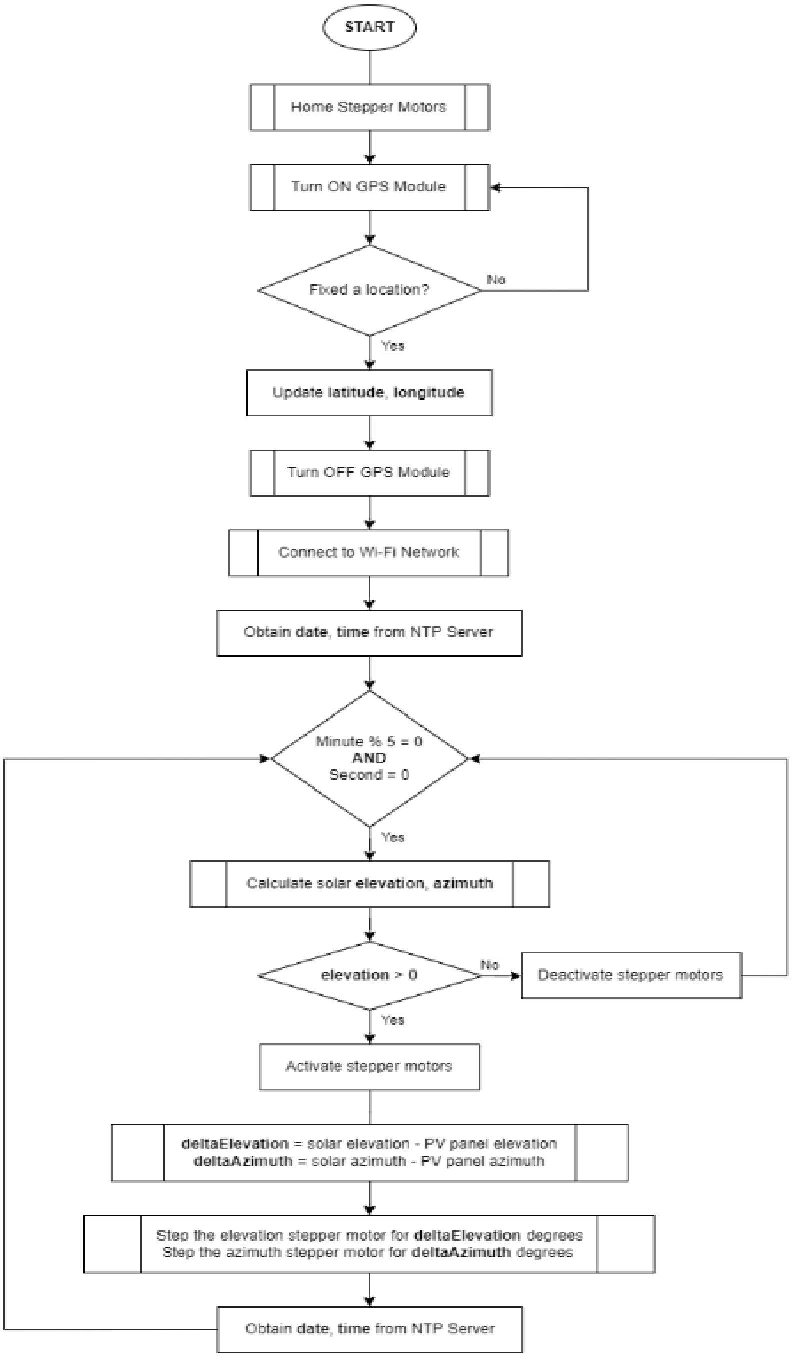

Fig. 20. Overall system flow chart for solar tracking system.

The system then checks whether the current minute is a multiple of 5 by calculating the appropriate modulo (minute % 5) before proceeding with the remaining steps in the program. In this way, solar tracking is executed at 5-minute intervals (i.e., whenever the current minute is a multiple of 5 at zero seconds). Solar tracking at intermittent intervals is feasible in this application as the sun moves at a very slow pace on the sky and continuous tracking every second would be futile. If the current minute is a multiple of 5 and current second is zero, the system proceeds with calculating the current solar elevation and azimuth angles using the solar position calculating algorithm that will be explained later. Next, the system checks whether the calculated elevation angle is greater than zero (i.e., whether the sun is above the horizon during daytime). If the elevation is a negative value, it indicates that the sun has already set; thus, the stepper motors are deactivated using the "sleep" pins on the motor driver. If the elevation is positive, the system proceeds to calculate the difference between the solar position angles and PV panel's position. Based on the difference, appropriate step commands are the sent for both stepper motor drivers to tilt and turn the PV panel in both axes as required. Once again, the current date and time are obtained, and the loop repeats as shown in the flowchart.

5. Electrical System Design

5.1. Electrical system investigation

MPPT algorithm in this case refers to Maximum Point Power Tracking (MPPT) algorithm where the algorithm is able to control the parameters of the PV panel in order to harvest the maximum power. To efficiently harvest the maximum power from the panel, the algorithm must constantly monitor the voltage/current/power of the panel based on the optimal operating voltage and current of the panel stated by the manufacturer on the datasheet.

Fig. **21** shows a sample datasheet of a PV module from Canadian Solar with the model number of CS32-430MS which is a 430 W PV panel. The focus here to achieve MPPT is by focusing the optimal operating voltage and current of the panel which is given by V_{mp} and I_{mp} with the rating of 40.3 V and 10.68 A in this case which total up to the maximum power of 430.404 W. Thus, a certain MPPT algorithm will be proposed to control the one or multiple parameters of the panel to achieve the MPP as long as possible throughout the day.

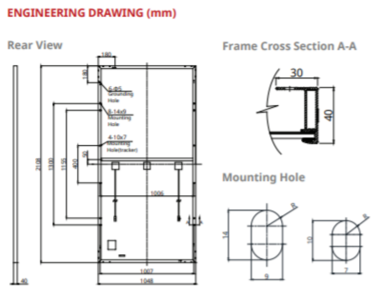

ELECTRICAL DATA | STC*

CS3W	430MS	435MS	440MS	445MS	450MS	455MS
Nominal Max. Power (Pmax)	430 W	435 W	440 W	445 W	450 W	455 W
Opt. Operating Voltage (Vmp)	40.3 V	40.5 V	40.7 V	40.9 V	41.1 V	41.3 V
Opt. Operating Current (Imp)	10.68 A	10.75 A	10.82 A	10.89 A	10.96 A	11.02 A
Open Circuit Voltage (Voc)	48.3 V	48.5 V	48.7 V	48.9 V	49.1 V	49.3 V
Short Circuit Current (Isc)	11.37 A	11.42 A	11.48 A	11.54 A	11.60 A	11.66 A
Module Efficiency	19.5%	19.7%	19.9%	20.1%	20.4%	20.6%
Operating Temperature	-40°C ~ +85°C					
Max. System Voltage	1500V (IEC/UL) or 1000V (IEC/UL)					
Module Fire Performance	TYPE 1 (UL 1703) or CLASS C (IEC 61730)					
Max. Series Fuse Rating	20 A					
Application Classification	Class A					
Power Tolerance	0 ~ + 10 W					

* Under Standard Test Conditions (STC) of irradiance of 1000 W/m², spectrum AM 1.5 and cell temperature of 25°C.

Fig. 21. Sample datasheet of CS32-430MS PV panel datasheet [10].

Going back to the electrical circuit of the system, in order to implement the MPPT algorithm and control the parameter of the panel, a circuit is needed as a medium to manipulate the set parameters in the panel. For such cases, a buck and/or boost converter will be used as the electrical medium.

Fig. **22** shows the different types of converters that can be implemented for the system. Fig. 22(a) shows a buck converter which is a converter that is able to step down the voltage from the source. Fig. 22(b) shows a boost converter which is a converter which step up the voltage and Fig. 22(c) shows a buck-boost converter which is a converter which can either step up or down the voltage from the source. In this case, the converter step-up or down ratio is depending on the duty cycle of the switching elements in the circuit and by controlling the duty cycle, we can achieve the MPP that were mentioned above.

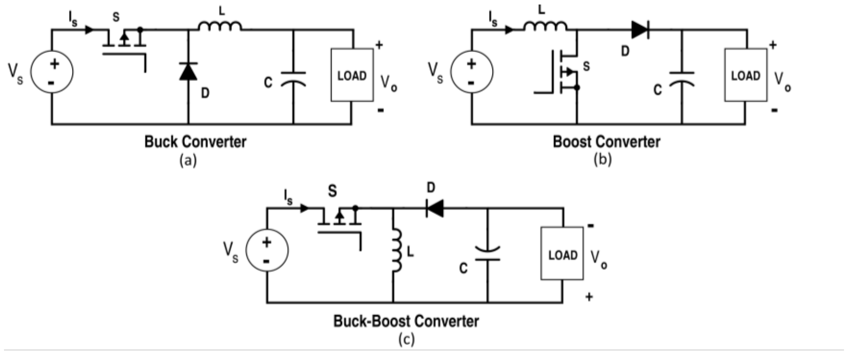

Fig. 22. DC-DC converters: (a) Buck. (b) Boost. (c) Buck-boost [11].

Other than that, if the panel is not storing its harvested energy in the battery due to the battery is fully charged or damaged, an inverter can be used as an interface to pump the harvested energy onto the city grid. Inverter is an electrical component that converts DC voltage to AC voltage and by precisely designing the inverter with a help of a step-up transformer, the low DC voltage level of the panel can be raised to the high AC voltage level of the grid.

Fig. **23** shows the widely use DC-AC converters or inverters on the market where Fig. 23(a) shows a half-bridge inverter which inverts the DC signal by only using two switching and Fig. 23(b) shows a full-bridge inverter which inverts the DC signal by using four switches.

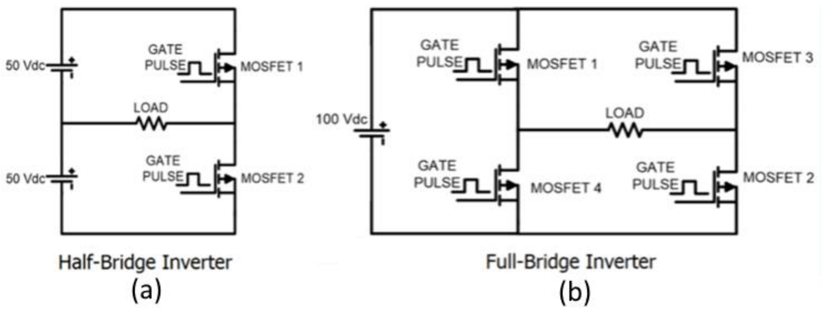

Fig. 23. DC-AC converters (inverters):
(a) Half-bridge inverter. (b) Full-bridge inverter [12].

5.2. Design of electrical system

Figure 24 shows the flowchart of electrical system that will be designed for the project. In this case, the start of the system will be the solar panel feeding its output power to the DC-DC converter and at the same time to the MPPT will be integrated into the DC-DC converter to extract its parameter out to the charge controller. The MPPT algorithm in this case will be either the constant voltage method or perturb and observe method. Even though the previous section selected the use of the constant voltage method, but the perturb and observe method will be tested in a simulation.

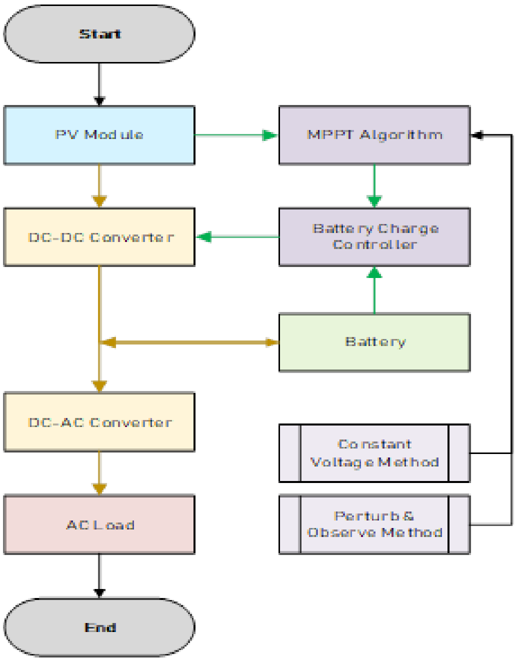

Fig. 24. Flowchart of electrical system.

The MPPT will then control the charge controller with the parameters of the battery which it will then manipulates the duty cycle of the DC-DC converter to achieve MPP and maintain a charging voltage for the battery. The battery or the output of the DC-DC converter will then power the DC-AC converter which converts the DC voltage to AC voltage which can be feed into the city grid or use to power the AC Load.

Fig. **25** shows the block diagram of the electrical system where it is similar to the flowchart of the system similar to Fig. 24.

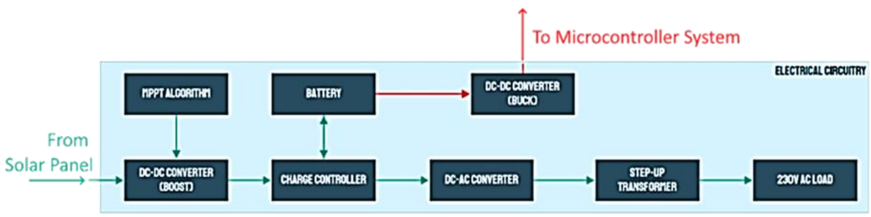

Fig. 25. Block diagram of electrical system.

6. Application and GUI Design

6.1. App and GUI design investigation

The implementation of IoT concepts has become a necessity in our everyday life. Automation has made its way into every task and has provided ease of completion. IoT implementation helps share the data for analysis and decision-making by the user. The communication of the sensors is stressed as it allows information sharing across multiple platforms [13].This chapter will focus on the implementation of an IoT dashboard which is able to constantly monitor, analyse and store the parameters recorded sent from the ESP 32 microcontroller via Wi-Fi.

This section encompasses the GUI design in the form of a mobile application that will be able to do all the tasks mentioned above. This application was created using Blynk which was designed for IoT based projects to control the hardware remotely, it can also display sensor data and store it as well. There are three elements in Blynk which are the application GUI itself which allows for dashboard creation and management. Then there is the Blynk server which enables the communication between the mobile device and the ESP 32. The option to run on a private Blynk server is also available otherwise the Blynk Cloud is available for everyone as it is open source. Lastly, the Blynk libraries are able to provide server connections and can process bidirectional commands.

Fig. **26** shows the main feature flow for Blynk. GUI implementation is needed to make sure that the user can monitor the different variables of the project to make sure that it is working properly along with analysing the parameters for future considerations. This eliminates the need for physical presence and is able to show us future contingencies within our project as well through its variable widgets. Blynk uses virtual pins to assign different GPIO pins to widgets inside the application using Virtual pins. For ESP 32 there are 32 usable virtual pins whereas they can be increased to 128 depending on the microcontroller using a special command in the Arduino sketch. In our project, we aim to connect the mobile application to the microcontroller using Wi-Fi and feed the inputs from the solar panel and battery into the application.

Error! Reference source not found. shows the main flow of how the application w ill get its data. We can see that the voltage sensor and current sensor will take inputs from the solar panel and battery which are their respective current and voltage values. The temperature sensor will take the solar panels temperature as input as well. All of this data will be sent to the ESP 32 microcontroller which will communicate with the Blynk app through Wi-Fi.

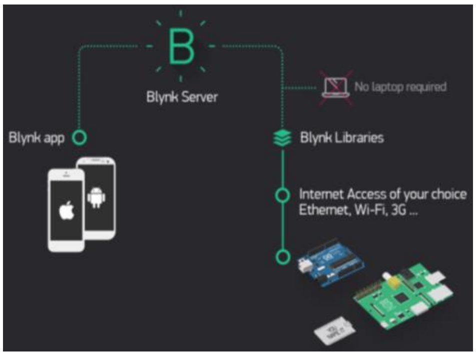

Fig. 26. Blynk feature flow.

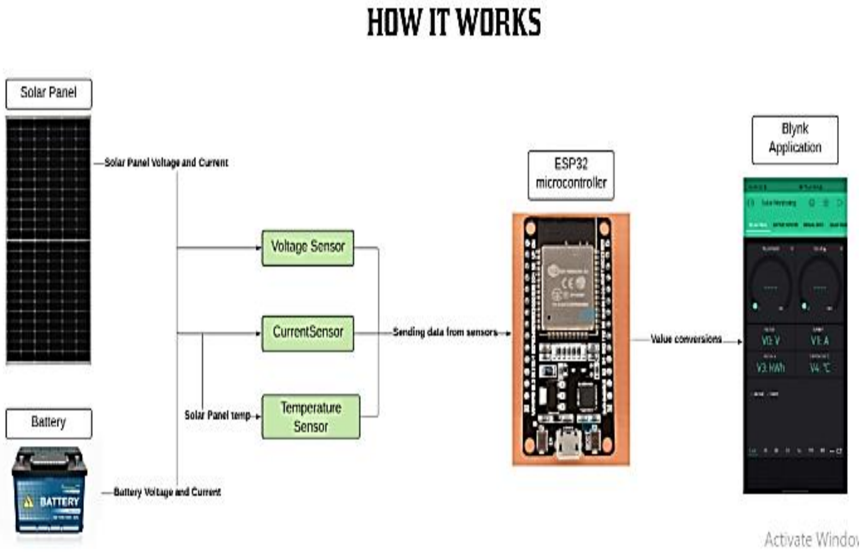

Fig. 27. Block diagram for blynk flow.

6.2. Design of GUI system

The main flow of this data acquisition system relies on the sensors for data to be sent to the ESP32 microcontroller which will then in turn communicate with the Blynk application, as shown in Fig. 28. The GPS module also provides locational data to the ESP32 which sends this over to the app as well. The current sensors use the Hall effect principle to measure the panel current and battery current which are assigned to the GPIO pins 14 and 33 respectively. These were translated to the virtual pins in the application assigned to their respective displays. The same method was used for the panel voltage and battery voltage assigned to the GPIO pins 35 and 34 respectively. The battery voltage panel was used to find the battery percentage level and display it using a gauge for better representation. The GPS module as discuss previously will provide accurate latitude and longitude values which were also assigned to their respective virtual pins to allow for the map widget to be able to display the real-time location from anywhere around the world.

The Blynk application is coded to show the solar power and energy harvested from the PV panel. It is also able to show savings based on the cost per kilowatt hour and converting to watt/hour for our prototype. We also have an integrated live super chart which maps the panel voltage and power to show consumption against output from the panel. There is a separate tab for battery monitoring which includes a battery percentage gauge alongside its voltage status also mapped onto a live graph. The last tab included into the application is for the solar tracker where it is able to show the real time location of the system based on the latitude and longitude provided from the GPS module. The azimuth and tilt values are also taken from previous section calculations to be represented onto the application. The angle deviation for specific times is charted via a graph. Manual inputs were also available, but our group decided to remove manual inputs as everything being automated would be much better overall.

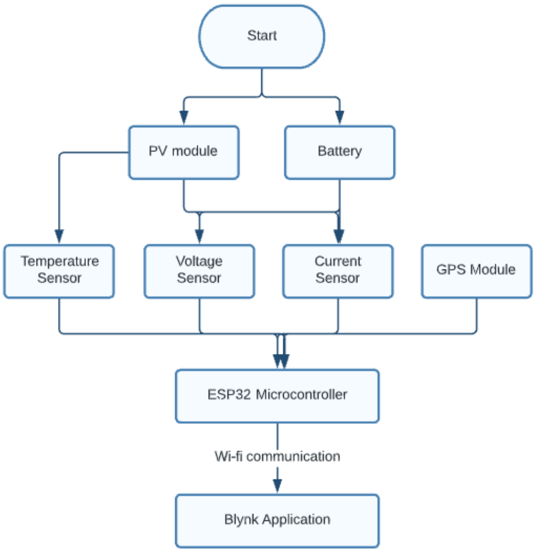

Fig. 28. Flow chart of system with Blynk.

7. Final Prototype

Fig. **29** shows the overall integrated system picture with all the integration and enhancement done onto the prototype. In this case, the middle picture shows the PV panel with the motorized platform which is 3D printed using PLA filament. Starting from the upper left and upper right, the two images show the passive cooling and active cooling for the prototype which include the heatsink and two 8 cm DC fan. Then the entire ESP32 microcontroller system actual circuit board is shown where the individual components were written on the picture. For the double helical gear and counterweight design, those two are the enhancement done onto the system to improve its performance. Lastly, the MPPT charge controller can be observe at the mid-bottom and the Blynk application which is the IoT-based application developed is shown at the mid-left.

Fig. 29. Integrated system overall pictures.

Fig. **30** shows the overall block diagram for the integrated system. Starting from the solar panel, it will first feed its power to the DC-DC converter where the converter will be controlled with a MPPT algorithm chip. The converter then feed the MPP power to the charge controller and the controller will regulate the power to charge the battery. The battery will then power a DC load and the extra charges will be fed into a DC-DC buck converter which it will lower the battery voltage from 12 V to 5 V to power the integrated system. The integrated system's main control will be from the ESP32 module as all the sensors and actuators will be controlled by the microcontroller. The solar tracking algorithm as well as the necessary coding to monitor the active cooling of the panel is uploaded onto the microcontroller.

The microcontroller then collects data from the GPS module and internet to then decide the input for the motor drivers which control the stepper motors to its turn to the accurate tilt and azimuth on the motorized platform. It will also collect the data from the thermistor that is connected at the back of the panel to then determine the control for the relay which turn on and off the DC fan for active cooling. Lastly, the data collected from the voltage and sensor module, as well as the cooling and solar tracking data will be fed to the IoT platform which consist of an application and GUI for the user.

The integrated system has solar tracking capability with GPS and a cooling system for the solar panel which is triggered by a temperature sensor. For none integrated systems both these features are not available.

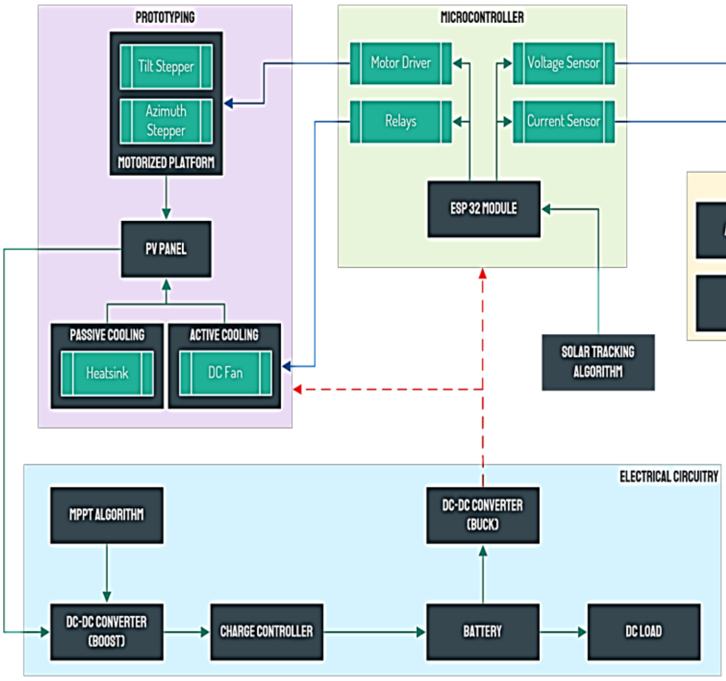

Fig. 30. Overall block diagram of integrated system.

7.1. Testing and results of prototype

Fig. **31** shows the integrated system solar data for 3 days with the continuous enhancement.

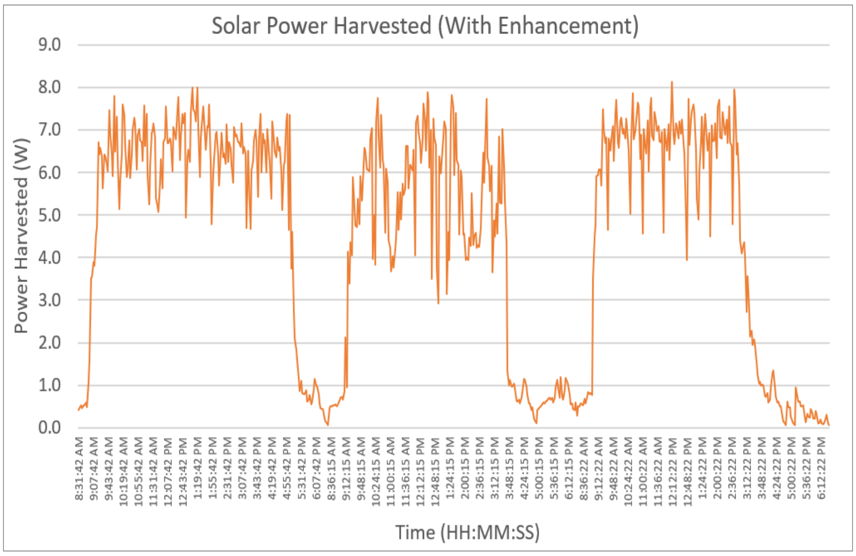

Fig. 31. Integrated system solar data with continuous enhancement.

Fig. **32** shows a similar PV panel solar data without any integrated enhancement which the data will be used to observe the efficiency increment of the integrated system.

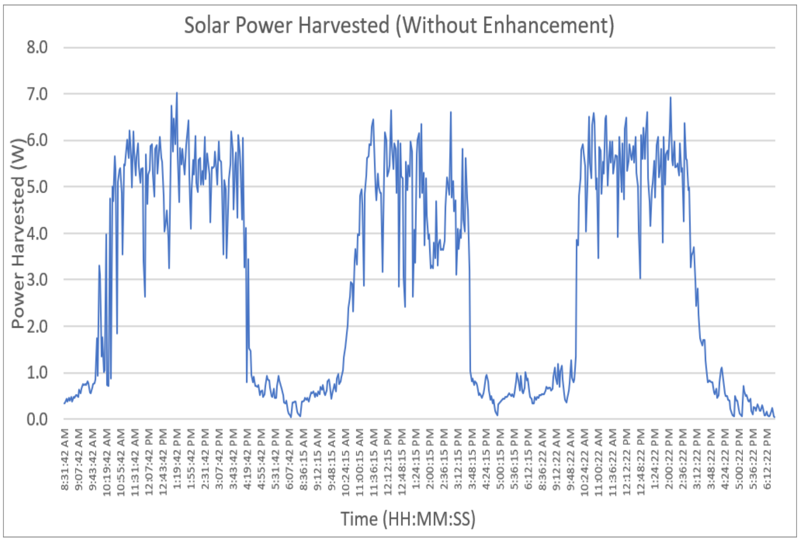

Fig. 32. Normal PV panel without any integrated enhancement.

Fig. **33** shows the comparison of solar data between the continuous enhancement shown in Fig. 31 and the similar PV panel without enhancement shown in Fig. 32. In this case, we can observe that the continuous enhancement greatly increases the average solar energy harvested which the benefit of solar tracking can be clear seen around morning (9am to 11am) and evening (4pm to 6pm). The efficiency increment of the integrated system is recorded as 49.57%.

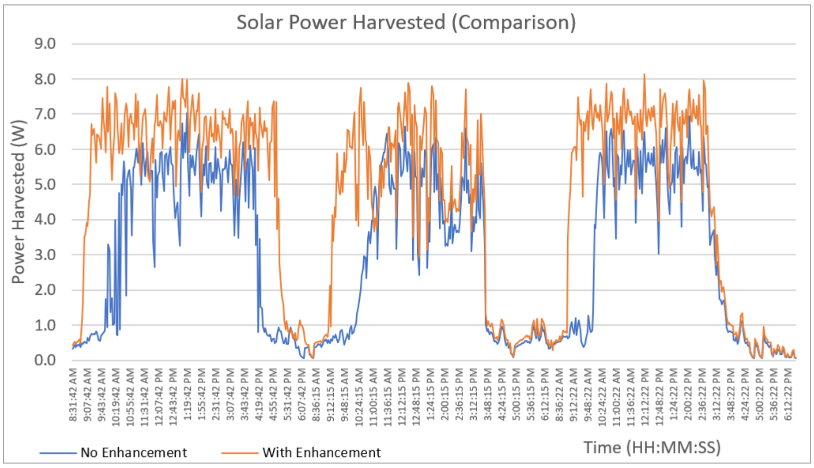

Fig. 33. Comparison of continuous enhancement and no enhancement.

Fig. **34** shows the comparison of solar data between the nett continuous enhancement and the similar PV panel without enhancement. In this case, the nett continuous enhancement refers to the data from the continuous enhancement, but it is subtracted with the energy consumed by the integrated system. For the power consumption of the integrated system, the stepper motor consumed 1.2 W, the DC fan consumed 1 W and the microcontroller consumed 0.5 W, which result in a total of 2.7 W power consumption when all integrated system is activated. The efficiency increments of the integrated system which recorded as 49.57% in the continuous enhanced system drops to only 1% after the subtraction.

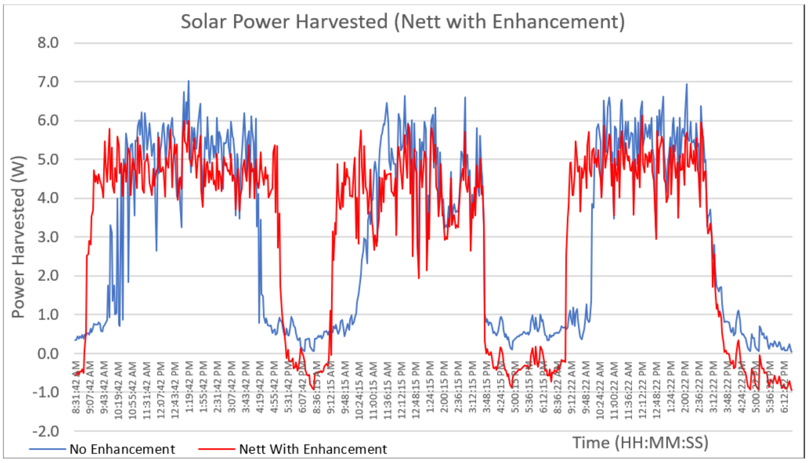

Fig. 34. Comparison of Nett continuous enhancement and no enhancement.

Error! Reference source not found. shows the comparison of solar data between t he conditional enhancement and similar PV panel without enhancement. In this case, the conditional enhancement is a solution to tackle the high-power consumption of integrated system, which it will only power the integrated system during the critical timing of the day. In this case, we can observe from Fig. 33 that the solar tracker provides the best result only on the certain timing during morning and evening, thus the microcontroller is coded with additional algorithm in which it will only power the stepper motor during those critical timing and also shut down the entire system if the power gets too low. The scenario of power getting too low before sunset can be clearly observed in day 2 and day 3 due to the weather condition (raining). In this case, the power drops around 4pm for both day and the system will intelligently shut off the integrated system to prevent unnecessary consumption during those conditions.

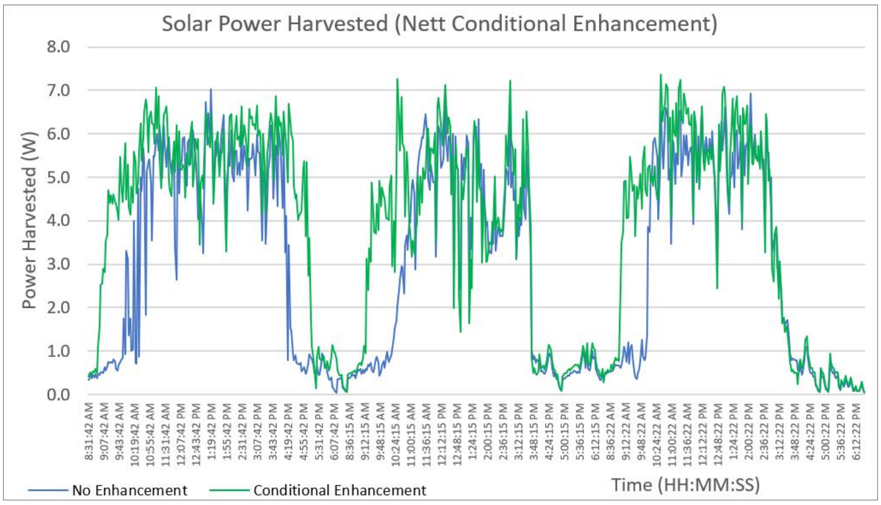

Fig. 35. Comparison of conditional enhancement and no enhancement.

8. Conclusions

In conclusion, the group project with the title of smart energy performance improvement on PV system was completed with full design process, simulated testing, prototype testing, results collection and evaluation and proper discussion and analysis. As a summary, the result indicated that the enhancement applied to the PV panel increases the PV panel efficiency by 49.57% and the IoT-based application on Blynk platform was successfully developed and able to monitors the parameters of the system in real time. However, the continuous solar tracking and powering the integrated system consumed additional power and lowered the efficiency by up to 48%. Anyhow, the issue was solved by integrating conditional algorithm into the controller which only turn on the integrated system during critical timing and the enhancement manage to retain at least 25.22% efficiency increment. Lastly, the project prototype also required a high cost of RM373.80 (at 2021) to developed in which was alleviated by innovative modifications such as cheaper stepper motor and only uses the microcontroller chip instead of the development board.

Acknowledgment

We have taken a lot of effort into this project. However, completing this project would not have been possible without the support and guidance of a lot of individuals. We would like to extend our sincere thanks to all of them. We are highly indebted to Mr. Suresh Gobee for his guidance and supervision. We would like to thank him for providing the advisory steps and direction to accomplish the project. We would also like to express our gratitude to Asia Pacific University for giving us the opportunity to complete the project. We are also very grateful to our parents and our friends for their kind co-operation and encouragement, which help us a lot in completing this project. Our thanks and appreciations go to our colleagues in developing the project. We deeply appreciate all the people who have willingly helped us out with their abilities.

References

1. Kurpaska, S.; Knaga, J.; Latala, H.; Sikora, J.; and Tomczyk, W. (2018). Efficiency of solar radiation conversion in photovoltaic panels. *Contemporary Research Trends in Agricultural Engineering*, 10.
2. Kazem, H.A.; Chaichan, M.T.; Alwaeli, A.H.; and Mani, K. (2016). *Mediterranean Green Buildings & Renewable Energy*. Chapter: Effect of Shadows on the Performance of Solar Photovoltaic. Springer, 379-385.
3. Srinivasan, K.G.; Vimaladevi, K.; and Chakravarthi, S. (2016). Solar energy monitoring system by IOT. *International. Journal. of Advanced Networking and Applications (IJANA)*, 46-51.
4. Honsberg, C.; and Bowden, S. (2020). Effect of temperature. Retrieved October 15, 2021, from https://www.pveducation.org/pvcdrom/solar-cell-operation/effect-of-temperature.
5. Energysage. (2021). How hot do solar panels get? Effect of temperature on solar performance. Retrieved November 3, 2021, from https://news.energysa ge.com/solar-panel-temperature-overheating/.
6. Ecogreenenergy. (2021). Temperature coefficient of solar pv module. Retrieved November 5, 2021, from https://www.eco-greenenergy.com/temperature-coefficient-of-solar-pv- module/.
7. MyGovernment. (2016). Climate. Retrieved November 16, 2021, from https://www.malaysia.gov.my/portal/content/144.
8. Zhang, H.; Sun, Y.; Wu, L.; Zhang, X.; and Xiang, Y. (2016). Tracking mechanism and cosine effect study of Module-Heliostat Solar. *Proceedings of the 2016 4th International Conference on Machinery, Materials and Information Technology Applications*. Xian, China.
9. Sampaio, P.G.V.; and González, M.O.A. (2017). Photovoltaic solar energy: Conceptual framework. *Renewable and Sustainable Energy Reviews*, 74, 590-601.
10. CanadianSolar. (2020). HiKu super high voltage module (430 W ~ 455 W) datasheet. Canada: Canadian Solar Inc.
11. EditorialTeam. (2015). Analysis of four DC-DC converters in equilibrium. Retrieved November 30, 2021, from https://www.allaboutcircuits. com/technical-articles/analysis-of-four-dc-dc-converters-in-equilibrium/.
12. Kansagara, R. (2019). Single phase half bridge and full bridge inverter using MATLAB. Retrieved November 29, 2021, from https://circuitdigest.com/ electronic-circuits/single-phase-half-bridge-and-full-bridge-inverter-circuit-using-matlab.
13. Saravanan, K.; Julie, E.G.; and Robinson, Y.H. (2018). Smart cities & iot: evolution of applications, architectures & technologies, present scenarios and future dream. *Internet of Things and Big Data Analytics for Smart Generation*, 135-151.